Modeling the Crossover between Chemically and Diffusion-Controlled Irreversible Aggregation in a Small-Functionality Gel-Forming System

S. Corezzi,*,† D. Fioretto,† C. De Michele,‡ E. Zaccarelli,‡,§ and F. Sciortino‡,§

Dipartimento di Fisica, Università di Perugia, Via A. Pascoli, I-06100 Perugia, Italy, and Dipartimento di Fisica and CNR-ISC, Università di Roma "La Sapienza", Piazzale A. Moro 2, I-00185 Roma, Italy

Received: November 24, 2009; Revised Manuscript Received: February 4, 2010

The analysis of realistic numerical simulations of a gel-forming irreversible aggregation process provides information on the role of cluster diffusion in controlling the late stages of the aggregation kinetics. Interestingly, the crossover from chemically controlled to diffusion-controlled aggregation takes place well beyond percolation, after most of the particles have aggregated in the spanning network and only small clusters remain in the sol. The simulation data are scrutinized to gain insight into the origin of this crossover. We show that a single additional time scale (related to the average diffusion time) is sufficient to provide an accurate description of the evolution of the extent of reaction at all times.

I. Introduction

Irreversible bonding of elementary units with a finite functionality f into branched clusters and networks is common to molecules, proteins, and colloidal particles, under the name of polymerization, irreversible aggregation, or clustering. The kinetics of cluster formation is sensitive both to the intrinsic rate of the chemical reaction process between clusters at contact and to the transport limitations that arise from the cluster size dependence of the diffusion coefficient. According to the relative importance of these two factors, the aggregation process is said to take place in the chemically controlled or diffusion-controlled limit. In general, the final structure of the aggregates results from a balance between the cluster size dependence of the diffusion process and the probability to irreversibly stick. It often happens that a transition from the chemically controlled to the diffusion-controlled limit occurs gradually as the aggregation product decreases the diffusivities in the system. Many thermoset materials of widespread use are the result of reactions where such crossover takes place.

A significant amount of theoretical work has focused on the description of the kinetics of irreversible aggregation,[1−5] mostly starting from the Smoluchowski coagulation equation,[6] describing the time evolution of the cluster size distribution $c_k(t) \equiv N_k(t)/V$

$$\frac{dc_k}{dt} = \frac{1}{2}\sum_{i+j=k} k_{overall}^{i,j} c_i c_j - \sum_{j=1}^{\infty} k_{overall}^{k,j} c_k c_j \qquad (1)$$

where $N_k(t)$ is the number of clusters of size k present in the system at time t, V is the volume, and the coagulation kernel $k_{overall}^{i,j}$ represents the rate coefficient for a specific clustering mechanism between clusters of sizes i and j. It is assumed that both intrinsic chemical constraints and diffusional limitations to the bonding can be taken into account through appropriate modeling of $k_{overall}^{i,j}$.[6] In experimental studies, on the other hand, one often searches for a simpler description that excludes the information on the cluster size distribution and focuses only on the experimentally more accessible time dependence of the fraction p of formed bonds, a measure of the extent of reaction. In the hypothesis that all sites have equal reactivity, independent of the size of the cluster to which they are attached, the fraction of formed bonds as a function of time, $p(t)$, satisfies

$$\frac{dp}{dt} = k_{overall}(1 - p)^2 \qquad (2)$$

where $k_{overall}$ is an overall rate coefficient of forming a single bond that incorporates all information on the aggregation process and that can, in general, depend on p. Equation 2 simply states that the probability to form a bond depends on the probability of encounter between two unreacted sites, independently of their spatial location or local environment. Equation 2 can also be derived from eq 1 by assuming that (i) the size dependence of $k_{overall}^{i,j}$ is not affected by diffusion but is completely determined by the product of the number of unreacted sites on clusters of size i and j and (ii) closed loops of bonded particles are absent.[7] In the chemical limit, $k_{overall}$ is constant (we indicate this constant value as k_c) and the solution of eq 2 with $p(0) = 0$ (i.e., starting from absence of bonds) is

$$p(t) = \frac{k_c t}{1 + k_c t} \qquad (3)$$

In general, how to best model the time (or p) dependence of the kernels $k_{overall}^{i,j}$ in eq 1 and $k_{overall}$ in the description of eq 2 is an open question.

Recently, we introduced a model for describing the irreversible aggregation process of a stoichiometric mixture of ellipsoidal particles of different sizes interacting through short-range directional interactions,[8,11] explicitly designed to simulate three-dimensional step-growth polymerization.[12] The model can also be considered representative of systems with bioselective interactions,[13,14] associating polymers,[15−17] functionalized mol-

* To whom correspondence should be addressed. E-mail: silvia.corezzi@fisica.unipg.it.
† Università di Perugia.
‡ Dipartimento di Fisica, Università di Roma "La Sapienza".
§ CNR-ISC, c/o Università di Roma "La Sapienza".

10.1021/jp911165b © XXXX American Chemical Society

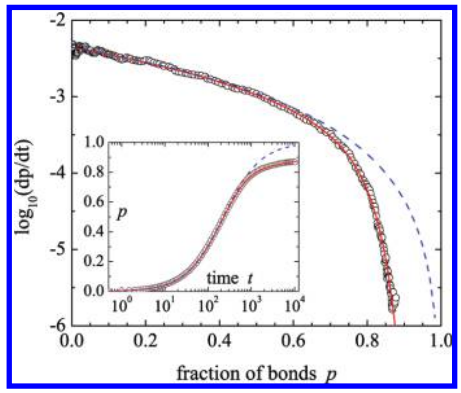

Figure 1. Rate of bond formation, dp/dt, as function of the fraction p of formed bonds. Symbols are the simulation results, averaged over 40 independent starting configurations up to $t \approx 10^3$ [in units of $\sigma(m/u_0)^{1/2}$] and over 11 configurations for longer times. The dashed and solid lines represent eq 2 in the chemically controlled limit [$k_{overall} = k_c = (4.43 \pm 0.01) \times 10^{-3}$, in units of inverse time] and in the case including the effects of diffusion ($k_{overall}$ given by eq 9), respectively. In the latter case, with k_c known from the early stages of aggregation and p_0 and γ known from the behavior of the diffusion coefficient (eq 6), the fit procedure adjusts only one parameter, $k_0 = 0.785 \pm 0.015$. Inset: Time dependence of the fraction of bonds p. Lines are solutions of eq 2 with the initial condition $p(0) = 0$, in the chemically controlled limit [dashed line; analytic solution (eq 3)] and in the case including the effects of diffusion (solid line; numerical solution).

ecules,[18] and patchy colloids.[19,20] Starting from an initial configuration of monomers, the aggregation process drives the formation of finite-size clusters (sol). The size of the clusters grows with time, progressively merging into an infinite (gel) cluster at the percolation transition when the bond probability reaches a critical value p_{gel}. At longer times, a final state is reached where essentially all particles belong to the infinite cluster, even if reaction has not reached its full extent [i.e., $p(\infty) \neq 1$]. It was found (see Figure 1) that $p(t)$ is well described by eq 3, with a constant value $k_{overall} = k_c$, up to $p \approx 0.65$, well beyond percolation. Furthermore, the cluster size distribution observed in the simulations during the aggregation process was compared to the corresponding quantity evaluated according to the Smoluchowski equation (eq 1) for the chemically controlled case, for which an analytic solution is available under the hypothesis of absence of bond loops in the aggregates of finite size.[7] It was found that, again for $p \lesssim 0.65$, the cluster size distribution calculated numerically coincides with the theoretical predictions (see Figure 3 of ref 8 and, for small clusters, Figure 2 of the present article).

In this article, we capitalize on the available simulations to investigate the reasons for the breakdown of the chemical limit. To do so, we analyze the evolution during polymerization of the diffusion properties of the system as well as of the clusters as a function of their size. The reported data can provide a useful reference to devise appropriate approximations to eq 1 incorporating the diffusion process. We finally show that a simple modeling of $k_{overall}$ in eq 2, taking into account the average diffusivity of the sites, is sufficient to provide an accurate description of the time evolution of $p(t)$ throughout the reaction.

II. Simulation Details, the Model, and a Brief Review of Its Properties

The model, introduced in ref 8, represents two types of mutually reactive molecules, A and B, as hard homogeneous ellipsoids of revolution whose surfaces are decorated in a predefined geometry by $f_A = 5$ and $f_B = 2$ identical reactive

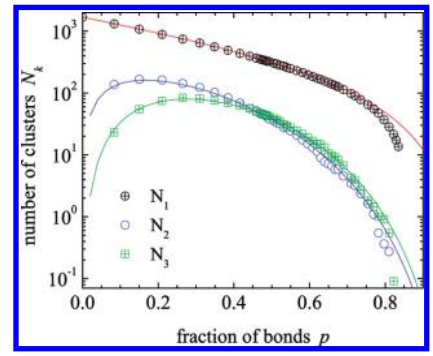

Figure 2. Number of monomers (N_1), dimers (N_2) and trimers (N_3), observed as a function of the fraction of formed bonds. Lines are the theoretical predictions of the Smoluchowski equation with kernels derived in the chemically controlled limit of the aggregation and absence of loops in finite size clusters (eq 4).

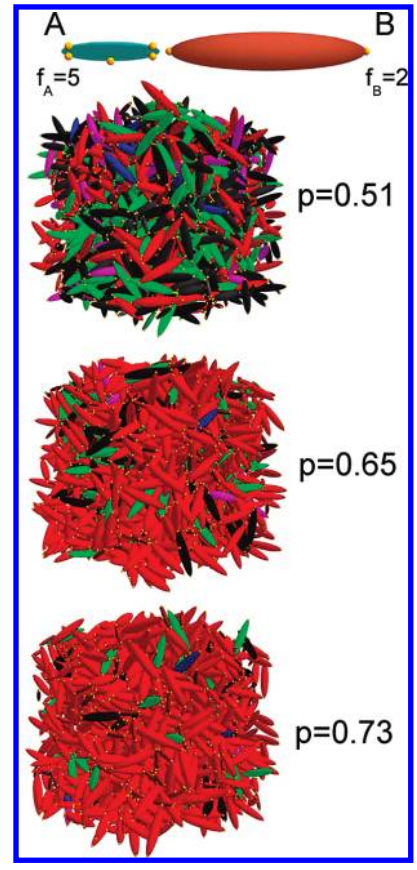

Figure 3. Graphical representation of A and B particles of the simulated system. Reactive sites are shown as orange spheres on the surface of the hard-core ellipsoidal particles. The other three panels show a pictorial representation of the system, in which the percolating cluster is colored in red, monomers in green, dimers in blue, trimers in magenta, and larger finite clusters in light black, at $p = 0.51$, 0.65, and 0.73 (i.e., above the percolation threshold $p_{gel} \approx 0.5$).

sites. The two molecules involved in the reaction are pictorially represented in Figure 3. Calling σ the unit of length and m the unit of mass, A particles are small and light (axes $a = 10\sigma$, $b = c = 2\sigma$, volume $V_A = 20\sigma^3/3\pi$, and mass $M_A = m$), whereas B particles are large and heavy (axes $a = 20\sigma$, $b = c = 4\sigma$, volume $V_B = 160\sigma^3/3\pi$, and mass $M_B = 3.4m$). Sites on particles of different type interact through an attractive potential that we model as a square well of depth $u_0 = 1$ and interaction range $\delta = 0.2\sigma$. Using event-driven molecular dynamics simulations, we study a binary mixture composed of $N_A = 480$ ellipsoids of type A and $N_B = 1200$ ellipsoids of type B. Because $f_A N_A =$

$f_B N_B$, the reactive sites of type A and B are initially present in equal numbers. This allows, in principle, the formation of a fully bonded state in which all of the sites have reacted. Time t is measured in units of $\sigma(m/u_0)^{1/2}$. The packing fraction is fixed at $\phi = 0.3$, which is a realistic value for a stoichiometric mixture of bifunctional diglycidyl ether of bisphenol A (B particles) with pentafunctional diethylenetriamine (A particles), the experimental system that inspired the model.[12]

A detailed description of the event-driven algorithm for rigid bodies interacting with additional site−site square-well potentials can be found in refs 9 and 10. In the numerical code, two mutually reactive sites i and j, on two distinct ellipsoids, form a bond if, during the dynamic evolution, the site−site distance r_{AB}^{ij} becomes smaller than δ. Once this condition is reached, the bond is formed, and bond formation is made irreversible by switching on an infinite barrier at distance $r_{AB}^{ij} = \delta$ between the sites i and j involved, which prevents both the breaking of the bond and the formation of additional bonds by the same sites. Between bond formation and collision events, all particles in the system propagate at constant translational and rotational velocities, with an average translational and rotational kinetic energy corresponding to a temperature $T = 1.0$. We note that the T value in the present simulations sets only the time scale for the exploration of phase space.

Because the site−site interaction potential is of a square-well form, there is no ambiguity in the number of bonds in the system, and hence, it is straightforward to evaluate the extent of reaction p as the ratio between this number and the maximum number of possible bonds $f_A N_A$. Clusters are defined as groups of bonded particles. Details on the connectivity properties of the model were reported in a previous publication,[8] where it was shown that the formation of bond loops within finite clusters (i.e., intracluster bonds connecting particles belonging to the same cluster) is negligible in this system throughout the aggregation process. The absence of loops in finite-size clusters is apparently favored by the elongated particle shape and the location of the reactive sites on the particle surface. For the present model, percolation was found at $p_{gel} \approx 0.5$ in agreement with the theory of Flory and Stockmayer,[21,22] which predicts a dependence of p_{gel} only on the functionality of the particles in the mixture $\{p_{gel} = 1/[(f_A - 1)(f_B - 1)]^{1/2}\}$ and not on the packing fraction. For completeness, we note that a ϕ-independent value of the bond probability along the percolation line has also been observed in a number of studies of patchy particle systems.[23−25]

In addition to the time dependence of p and the evolution of the cluster size distribution, ref 8 reported also a comparison with the predictions of mean-field theories for loopless aggregation. Here, we focus on the distribution of small-size clusters and on how their relative concentration changes with p, an element that will be relevant for the analysis reported in the next section. Figure 2 shows the numbers of monomers (N_1), dimers (N_2), and trimers (N_3) in the system as functions of the extent of reaction. We observe that the number of monomers exceeds the number of dimers by more than 1 order of magnitude throughout the explored time window. The figure also shows the corresponding predictions of the Flory−Stockmayer model (also solutions of the Smoluchowski equation in the loopless chemically controlled limit), namely

$$\begin{aligned} N_1 &= N_A(1-p)^5 + N_B(1-p)^2 \\ N_2 &= \frac{20N_A N_B}{5N_A + 2N_B}p(1-p)^5 \\ N_3 &= 4N_B p^2(1-p)^5 + \frac{5}{2}N_A p^2(1-p)^8] \end{aligned} \tag{4}$$

The theoretically predicted values of N_k agree very well with the numerical data for $p \lesssim 0.65$, that is, well above the percolation threshold p_{gel}. The breakdown of the chemical approximation thus manifests itself simultaneously in the time evolution of p and in the departure of N_k from the Flory−Stockmayer predictions. Figure 2 also shows that the number of monomers significantly drops upon increasing p beyond p_{gel}, but at a lower rate than for larger clusters, quickly becoming the dominant particles in the sol. Hence, at large values of p, the percolating cluster coexists with sol particles, which are mostly found in monomers and very small aggregates. To provide a graphical visualization of the system structure and clustering in the large-p region, we show in Figure 3 configurations at three different values of p, all above p_{gel}. It appears clearly that the sol concentration is strongly suppressed with increasing p and that only very small clusters are present in the region where the chemical approximation breaks down.

III. Results

To understand the failure of eq 3 for $p \gtrsim 0.65$ (Figure 1), we investigate the diffusion processes in the system. We start by examining the system's diffusivity properties for each studied value of p. Figure 4a shows the overall diffusion coefficient, evaluated as

$$D = \lim_{t\to\infty}\langle \Delta r^2(t)\rangle/6t \tag{5}$$

where $\langle \Delta r^2(t)\rangle = \langle \sum_{i=1}^{N} \Delta r_i^2(t)/N\rangle = \langle \sum_{i=1}^{N} |\vec{r}_i(t) - \vec{r}_i(0)|^2/N\rangle$ is the mean squared displacement of all the particles in the system over the time period t. Here, $\langle \cdot \rangle$ denotes an ensemble average, $\vec{r}_i$ is the position vector of particle i, and i labels the $N = N_A + N_B$ particles of the system. To provide an accurate determination of D that is not affected by the ongoing polymerization process, we exploit the possibility offered by the numerical simulation of freezing the aggregation process and analyzing the dynamics in a system of fixed cluster-size composition. More precisely, during the simulation, when a given value of p is achieved, the positions and velocities of all particles are copied and used to start a new simulation in which the bonding pattern is frozen by switching on an infinite barrier at distance δ between each pair of mutually reactive sites. In this new simulation, the formed clusters remain free to move while retaining their integrity (i.e., not binding to other clusters), and D is calculated from the long-time limit of $\langle \Delta r^2(t)\rangle$, evaluated where possible subdiffusive behavior is over and a linear increase in time is established. This simulation protocol also allows us to evaluate, with sufficient numerical accuracy, the diffusion coefficient of small clusters and to assess its dependence on the cluster size. An average over 11 independent realizations was performed to improve the statistics.

The numerical results for the p-dependent evolution of D are well described by a power law

$$D = D_0\left(\frac{p_0 - p}{p_0}\right)^{\gamma} \tag{6}$$

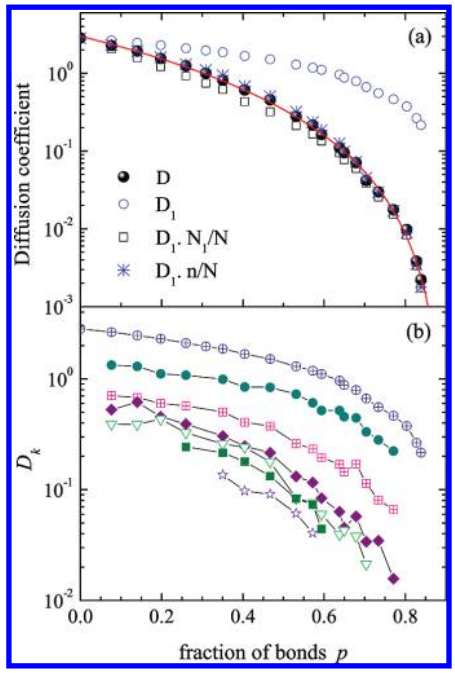

Figure 4. (a) Overall diffusion coefficient, D (●), and diffusion coefficient of monomers, D_1 (○), as functions of the fraction of bonds p. Open squares represent the monomer contribution to the overall diffusion coefficient, D_1N_1/N. Stars represent the overall diffusion coefficient evaluated, in the approximation of Stokesian diffusion of the clusters, as $D \approx D_1 n/N$, where $n = \sum_k N_k$ counts the total number of clusters and N is the number of particles in the system. The solid line is the best fit of $D(p)$, using eq 6. (b) Dependence on p of the average diffusion coefficient of k-mers, for $k = 1, 2, ..., 7$ from top to bottom. In both panels, diffusion coefficients are measured in units of $\sigma(u_0/m)^{1/2}$.

where D_0 is the diffusion coefficient at $p = 0$, γ is the power-law exponent, and p_0 is the value of p where diffusion is expected to vanish. The best-fit values are $\gamma = 2.69 \pm 0.07$ and $p_0 = 0.902 \pm 0.005$. The power-law behavior of D recalls the analogous slowing of the dynamics in glass-forming liquids, where similar dependence of D on temperature, pressure, or packing fraction is seen close to the mode-coupling transition.[26] The value $p_0 \neq 1$ suggests that the arrest of the dynamics occurs before all available sites have reacted, that is, that a fraction of unreacted sites exists in the arrested gel network.

In the region where the chemical approximation starts to fail ($p \gtrsim 0.65$), most of the particles in the system belong to the infinite cluster (see Figure 4a in ref 8). The remaining material, the sol phase, is mostly constituted by small clusters, as seen in Figure 2. Hence, it is interesting to compare what fraction of the diffusion coefficient is provided by the motion of the N_1 clusters of size one (monomers). Figure 4 compares D with D_1N_1/N (open squares in Figure 4a) for all p values. Beyond $p \approx 0.65$, the diffusion process is mostly controlled by the diffusion of monomers.

Note that the overall diffusion coefficient D can also be written as $D = \sum_i D_i/N$, where $D_i = \lim_{t\to\infty}\langle \Delta r_i^2(t)\rangle/6t$ is the diffusion coefficient of particle i, or, equivalently, by grouping together all particles in clusters of the same size, as $D = \sum_k D_k k N_k/N$, where D_k is the average diffusion coefficient of clusters of size k and kN_k/N is the fraction of particles in the system that belong to k-size clusters. The cluster diffusion coefficient corresponds to the long-time limit of the mean squared displacement of the cluster center of mass, and it also is evaluated in a frozen-bond condition. Figure 4b shows the p evolution of D_k, up to $k = 7$. All D_k values show a clear slowing with increasing p. A power-law fit of D_k is possible for small

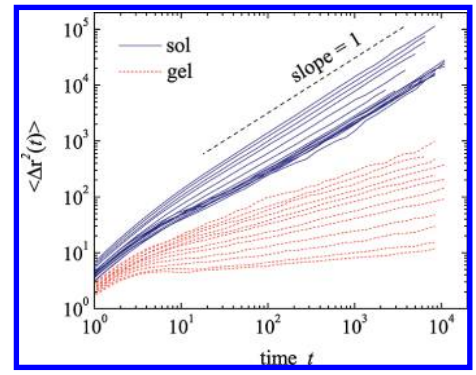

Figure 5. Mean squared displacements of sol and gel particles, for configurations at different fractions of formed bonds, increasing from top to bottom of each set of curves ($0 \le p \le 0.84$ for sol configurations, $0.53 \le p \le 0.84$ for gel configurations). A slope equal to 1 is expected when particles are diffusive.

k, providing evidence that, for all cluster sizes, the arrest of the dynamics occurs at a finite value of $p_0 \approx 0.88$, very close to (and within our numerical error of) the value found for the overall diffusion coefficient D.

Having evaluated D_k, we can also analyze the simulation data to test one of the commonly found approximations in the theoretical literature,[4,5] the assumption of a (p-independent) scaling relationship between the cluster size and the diffusion coefficient (i.e., $D_k = D_1 k^{-1}$), the so-called Stokesian limit of diffusion. In this approximation, we can write

$$D = \sum_k \frac{D_1}{k}\frac{kN_k}{N} = \frac{D_1}{N}\sum_k N_k = D_1\frac{n}{N} \qquad (7)$$

where $n = \sum_k N_k$ is the total number of clusters in the system. Equation 7 shows that the slowing of the overall diffusion arises from two different mechanisms: the decrease of the diffusion coefficient of the monomers and the decrease in the number of diffusing clusters. The difference between this expression and the one that takes only monomers into account (i.e., includes only the first term in the sum) can be assessed in Figure 4a. Even though the assumption of Stokesian dynamics for the clusters is clearly incorrect according to the data shown in Figure 4b, eq 7 provides an excellent description of D in the entire range of p. This agreement brings further evidence to the fact that D is controlled mostly by the small clusters, which are faster and more abundant, essentially determining the diffusional behavior of the system.

As an additional confirmation that the entire diffusion process is associated with the sol clusters, we show in Figure 5 the mean squared displacements for sol and gel particles for several values of p. The sol particles always retain a diffusive motion, whereas the large-scale motion of the gel is subdiffusive, that is, the mean squared displacement of the gel center of mass increases less than linearly in time. Moreover, the particles belonging to the gel network are always much more localized than the particles in the sol fraction (Figure 5). These results show that the gel contribution to the diffusion can be safely neglected.

The analysis of the size dependence of the cluster mobility allows us to comment on the conventional approach based on the Smoluchowski coagulation equation, where the cluster mass dependence of D_k is generally presumed not to change with the advancement of the reaction.[4,5] We show in Figure 6 how D_k scales with the mass of the cluster, M, for different values of p, by properly taking the different masses of the small and large

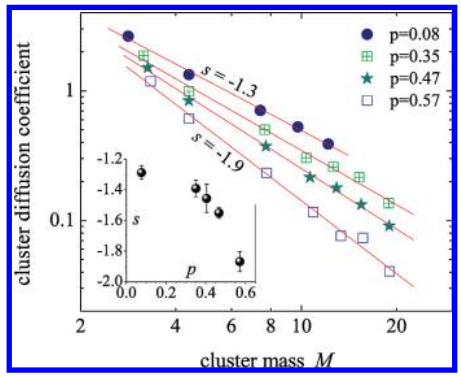

Figure 6. Diffusion coefficient of clusters as a function of their mass M, at different values of the bond fraction p, as indicated in the legend. Lines are the best fit to a power law $D \sim M^s$. The inset shows the p dependence of the exponent s.

particles into account.[27] The simulation data, compared with the expectation of a power law $D_k \sim M^s$,[28,29] provide different estimates of the s exponent for different values of p (see inset of Figure 6), revealing that a change in the structure of the environment in which branched clusters are moving has a significant impact on the size dependence of the cluster mobility. Note that D_k decreases faster than M^{-1} already in the initial stages of the reaction, and it decreases even faster for p increasing close to and beyond the gel point ($p_{gel} = 0.5$). The p dependence of the exponent highlights the difficulty of providing an accurate and detailed model of the aggregation process when diffusion is relevant, because it is not sufficient to postulate a time-independent coupling between the diffusion of clusters and their size.

IV. Discussion

The results presented in the previous section clearly show that the modeling of the long-time kinetics of aggregation for the investigated patchy ellipsoidal system does require the introduction of transport limitation contributions in the aggregation kernels. At the level of the less-demanding description of eq 2, an expression of $k_{overall}$ must also be devised that captures both the properties of the chemical bonding act and the diffusive properties of the clusters to which the reactive sites are attached. Following the Rabinowitch model for small-molecule reactions[30] and subsequent theoretical works,[31−33] we write

$$k_{overall}^{-1} = k_c^{-1} + k_{diff}^{-1} \tag{8}$$

where k_c is the intrinsic rate constant, which is given by the chemistry of the system, and k_{diff} is the rate coefficient for a system with no chemical barriers where reactions occur upon collision of functional groups. The latter rate constant depends on the diffusion time scale. Equation 8 simply states that the time required to form a new bond is the sum of the time required for two clusters of any size to approach each other plus the time required for repeated collisions between nearby clusters to become fruitful in providing a bond between the clusters. The parallel sum of k_c and k_{diff} suggests that, in the early stages of aggregation, when the system consists mainly of monomers and oligomers, the particle mobility is high and the aggregation proceeds in the absence of diffusional limitations ($k_{diff} \gg k_c$; hence, $k_{overall} \approx k_c$). However, as the extent of reaction is increased, the cluster-size dependence of the diffusion coefficient starts to limit the reactivity of unreacted sites, so that, for large values of p, the rate of aggregation is primarily determined by the mass transfer of the reactants ($k_{diff} \ll k_c$; hence, $k_{overall} \approx k_{diff}$).

Because the early-time kinetics is properly described by the Smoluchowski equation (as discussed at length in ref 8 and shown in Figure 1), the constant value of k_c [$= (4.43 \pm 0.01) \times 10^{-3}$, in units of inverse time] in this system is entirely determined by the early-time behavior of the aggregation. The case of k_{diff} is different, as it requires an ansatz for the p dependence of the diffusional time. In the spirit of the mean-field description of eq 2, we test the possibility that the diffusion rate constant is proportional to the average diffusion coefficient (eq 6), writing

$$k_{overall}^{-1} = k_c^{-1} + k_0^{-1}\left(\frac{p_0 - p}{p_0}\right)^{-\gamma} \tag{9}$$

where k_0 is an unknown constant.

A comparison between the simulation data for dp/dt versus p and eq 2 [with $k_{overall}(p)$ expressed by eq 9] offers a way to test the quality of the approximation and to extract the best value of k_0 as a single additional fit parameter. The best-fit value is $k_0 = 0.785 \pm 0.015$, in units of inverse time, that is, 2 orders of magnitude larger than k_c, thus providing a clear separation between the two kinetic regimes. The solid line in Figure 1 demonstrates that the diffusion-controlled rate equation derived in a mean-field approximation provides an excellent description of the entire kinetic process. The close agreement between the simulation and diffusion-corrected modeling is further stressed in the inset of Figure 1, comparing the numerical solutions of eq 2 with the initial condition $p(0) = 0$ in the cases of $k_{overall} = k_c$ and $k_{overall}$ given by eq 9.

The presence of a spanning irreversibly bonded network severely constrains the motion of the sol clusters of any size. As shown in Figure 4b, the cluster diffusion decreases by 1 order of magnitude during the aggregation process. An even larger effect is seen on the average diffusivity, which decreases by several orders of magnitude. Such a decrease is mostly driven by the progressive reduction in the number of clusters in the sol and, in the interesting kinetic region where diffusion effects are dominant, mainly by the change in the number of monomers. The higher diffusivity of the monomers results in a progressive depletion of small clusters as compared to the predicted concentration in the reaction-limited case (Figure 2). Discrepancies between the cluster size distribution observed in the simulation and that provided by the ideal kinetic theory of aggregation are therefore not easily dismissed as an effect associated with the omitted spatial information in the coagulation kernels. Instead, they are likely to be associated with the diffusion-altered size-dependent reaction rates, which favor the depletion of faster, small clusters and the reduced production of slower, large clusters.[4,34]

In the model investigated here, diffusional processes become relevant only for late stages of aggregation (i.e., $p \gtrsim 0.65$) and allow a facile modeling of the entire evolution of $p(t)$ simply accounting for the decrease of the system's average diffusivity (which, in itself, is driven by a decrease in the number of sol clusters). It is interesting to discuss why the chemical limit works for such a long interval, well beyond percolation. At the basis of this behavior is the small value of the chemical rate constant k_c (with respect to k_0). The origin of such a small value has to be found in the essence of the patchy interaction, which, thanks to its short-range nature and localization, imposes by itself an

entropic barrier to bond formation. Bonding indeed requires that two reactive sites become close to each other or, in equivalent terms, that the two reacting clusters face each other with the right orientation. In the present model, in which the bonding site−site distance is much smaller than the particle size, the time needed for two clusters to diffuse and approach each other is significantly smaller than the time required to orient themselves in the right bonding geometry. As a result, the model favors the establishment of a wide chemically controlled time region. The existence of such a wide region (up to $p \approx 0.65$) has the consequence that, when diffusion starts to become relevant, because of the general mechanism that the average distance between unreacted sites has grown, coupled with the increased size of the diffusing clusters, the sol clusters that contribute to diffusion are mostly monomers that progressively react with the infinite cluster, determining the faster depletion of their concentration mentioned above.

In this work, we have studied one single value of ϕ, corresponding to a realistic packing fraction for an epoxy-amine system.[12] We expect that similar results are found for different packing fractions, although the extent of the chemically controlled regime might change. Because the cluster diffusion coefficient will decrease with increasing ϕ, because of the increase of the system's viscosity, the crossover between $k_{overall} \approx k_c$ and $k_{overall} \approx k_{diff}$ will be affected, and the diffusion-controlled limit of the aggregation will set in for smaller values of p. Indeed, a previous study of irreversible polymerization at smaller values of packing fraction did not reveal any crossover to a diffusion-limited regime.[35] For very large ϕ, when polymerization may compete with excluded-volume-driven glass formation, more complicated scenarios can arise.

V. Conclusions

The results of this study clearly indicate that the effect of diffusional limitations on the kinetics of aggregation, in a realistic model of patchy particles, can be taken into account by introducing a single characteristic p-dependent time scale. This time scale and its dependence on the extent of reaction can be properly associated with the average diffusion time scale. This result has been made possible by the simultaneous determination of the extent of reaction as a function of time, $p(t)$, and of the diffusion coefficient as a function of the extent of reaction, $D(p)$. We have found that, with only one additional (p-independent) fit parameter, the entire evolution of $p(t)$ can be modeled, even in the last stages of aggregation, where a small number of finite clusters remain interspersed within the frozen structure of the gel network. The small particle functionality appears to be a key ingredient to shift the crossover between the chemically controlled and diffusion-controlled limits well beyond the percolation point,[35] when most particles belong to the infinite network and only small clusters remain in the sol.

We note in passing that, although the shape anisotropy of the particles is important for the present study to mimic stepwise polymerization of a realistic system,[12] this feature is not crucial for the validity of our results. In all cases where bond loops in finite-size clusters can be safely neglected, a situation that can be realized effectively also in a system of spherical particles with small average functionality,[36] the evolution of the extent of reaction can be modeled in a manner similar to that proposed here.

The present study also has potential relevance to experimental studies of step-growth polymerization, where the diffusion-controlled kinetics is analyzed by replacing each chemical rate constant with an overall one, built on the Rabinowitch model (eq 8) and the assumption of proportionality between k_{diff} and the overall diffusion coefficient.[37−41] The experimental approach suffers from certain limitations in order to assess its validity, as it relies on the knowledge of the kinetic equation governing the chemically controlled limit of the reaction, which, in most situations, is complicated by autocatalytic terms[42] or multiple-reaction effects[43] or is obtained on a semiempirical basis,[44] and on the determination of the diffusion coefficient, which, in most cases, cannot be directly accessed and requires a nontrivial assumption about the way it is related to the structural relaxation time measured experimentally.[39,45] The present patchy particle model does not suffer from ambiguity in the intrinsic chemical kinetics and permits a precise determination of the diffusion properties, thus offering the possibility to check, for the first time in a direct manner, the soundness of the approach employed to model diffusion control in experimental studies.

Acknowledgment. We acknowledge support from ERC-226207-PATCHYCOLLOIDS, EU-ITN COMPLOIDS, and SoftComp NMP3-CT-2004-502235. We thank P. Tartaglia for helpful discussions.

References and Notes

(1) Tulig, T. J.; Tirrell, M. *Macromolecules* **1981**, *14*, 1501.
(2) van Dongen, P. G. J.; Ernst, M. H. *Phys. Rev. Lett.* **1985**, *54*, 1396.
(3) van Dongen, P. G. J. *J. Stat. Phys.* **1997**, *87*, 1273.
(4) Oshanin, G.; Moreau, M. *J. Chem. Phys.* **1995**, *102*, 2977.
(5) Guzmán, J. D.; Pollard, R.; Schieber, J. D. *Macromolecules* **2005**, *38*, 188.
(6) von Smoluchowski, M. *Z. Phys. Chem.* **1917**, *92*, 129.
(7) van Dongen, P. G. J.; Ernst, M. H. *J. Stat. Phys.* **1984**, *37*, 301.
(8) Corezzi, S.; De Michele, C.; Zaccarelli, E.; Fioretto, D.; Sciortino, F. *Soft Matter* **2008**, *4*, 1173.
(9) De Michele, C.; Gabrielli, S.; Tartaglia, P.; Sciortino, F. *J. Phys. Chem. B* **2006**, *110*, 8064.
(10) De Michele, C. *J. Comput. Phys.* **2010**, *229*, 3276.
(11) Corezzi, S.; De Michele, C.; Zaccarelli, E.; Tartaglia, P.; Sciortino, F. *J. Phys. Chem. B* **2009**, *113*, 1234.
(12) Corezzi, S.; Fioretto, D.; Kenny, J. M. *Phys. Rev. Lett.* **2005**, *94*, 065702.
(13) Hiddessen, A. L.; Rodgers, S. D.; Weitz, D. A.; Hammer, D. A. *Langmuir* **2000**, *16*, 9744.
(14) Ghofraniha, N.; Andreozzi, P.; Russo, J.; La Mesa, C.; Sciortino, F. *J. Phys. Chem. B* **2009**, *113*, 6775.
(15) Ermoshkin, A. V.; Kudlay, A. N.; Olvera de la Cruz, M. *J. Chem. Phys.* **2004**, *120*, 11930.
(16) Loverde, S. M.; Ermoshkin, A. V.; Olvera de la Cruz, M. *J. Polym. Sci. B: Polym. Phys.* **2005**, *43*, 796.
(17) Olvera de la Cruz, M.; Ermoshkin, A. V.; Carignano, M. A.; Szleifer, I. *Soft Matter* **2009**, *5*, 629.
(18) He, G.; Tan, R. B. H.; Kenis, P. J. A.; Zukoski, C. F. *J. Phys. Chem. B* **2007**, *111*, 14121.
(19) Bianchi, E.; Largo, J.; Tartaglia, P.; Zaccarelli, E.; Sciortino, F. *Phys. Rev. Lett.* **2006**, *97*, 16830.
(20) Kraft, D. J.; Groenewold, J.; Kegel, W. K. *Soft Matter* **2009**, *5*, 3823.
(21) Flory, P. J. *Principles of Polymer Chemistry*; Cornell University Press: Ithaca, NY, 1953.
(22) Stockmayer, W. H. *J. Polym. Sci.* **1952**, *9*, 69.
(23) Bianchi, E.; Tartaglia, P.; La Nave, E.; Sciortino, F. *J. Phys. Chem. B* **2009**, *111*, 11765–11769.
(24) Largo, J.; Starr, F. W.; Sciortino, F. *Langmuir* **2007**, *23*, 5896–5905.
(25) Zaccarelli, E.; Sciortino, F.; Tartaglia, P. *J. Chem. Phys.* **2007**, *127*, 174501.
(26) Götze, W. *Complex Dynamics of Glass-Forming Liquids: A Mode-Coupling Theory*; Oxford University Press: Oxford, U.K., 2009.
(27) Note that the average mass of a k-mer is slightly different for different values of p, because of different contributions from small and large particles.
(28) Lodge, T. P. *Phys. Rev. Lett.* **1999**, *83*, 3218.
(29) Del Gado, E.; de Arcangelis, L.; Coniglio, A. *Eur. Phys. J. E* **2000**, *2*, 359.
(30) Rabinowitch, E. *Trans. Faraday Soc.* **1937**, *33*, 1245.
(31) Achilias, D. S.; Kiparissides, C. *Macromolecules* **1992**, *25*, 3739.
(32) Collins, F. C.; Kimball, G. E. *J. Colloid Sci.* **1949**, *4*, 425.
(33) O'Shaughnessy, B. *Macromolecules* **1994**, *27*, 3875.

(34) Cotts, D. B.; Berry, G. C. *Macromolecules* **1981**, *14*, 930.
(35) Sciortino, F.; De Michele, C.; Corezzi, S.; Russo, J.; Zaccarelli, E.; Tartaglia, P. *Soft Matter* **2009**, *5*, 2571.
(36) Russo, J.; Tartaglia, P.; Sciortino, F. *J. Chem. Phys.* **2009**, *131*, 014504.
(37) Boogh, L.; Mezzenga, R. Processing Principles for Thermoset Composites. In *Comprehensive Composite Materials, Vol. 2: Polymer Matrix Composites*; Elsevier Science: Amsterdam, 2000.
(38) Girard-Reydet, E.; Riccardi, C. C.; Sautereau, H.; Pascault, J. P. *Macromolecules* **1995**, *28*, 7599.
(39) Deng, Y.; Martin, G. C. *Macromolecules* **1994**, *27*, 5147.
(40) Wise, C. W.; Cook, W. D.; Goodwin, A. A. *Polymer* **1997**, *38*, 3251.
(41) Huguenin, F. C. A. E.; Klein, M. T. *Ind. Eng. Chem. Prod. Res.* **1985**, *24*, 166.
(42) Rozenberg, V. A. *Adv. Polym. Sci.* **1986**, *75*, 113.
(43) Cole, K. C. *Macromolecules* **1991**, *24*, 3093.
(44) Kamal, M. R. *Polym. Eng. Sci.* **1974**, *14*, 23.
(45) D is often assumed to be inversely proportional to the structural relaxation time τ. The relationship $D \sim \tau^{-1}$, however, is derived within the theory of macroscopic hydrodynamics, whose application in the slow dynamic regime has been found to fail in many systems. Deviations from the expected behavior have been described by $D \sim \tau^{-\xi}$, where ξ is a fractional exponent.

JP911165B